ORIGINAL ARTICLE

Lung Cancer Driven by BRAF^{G469V} Mutation Is Targetable by EGFR Kinase Inhibitors

Ku-Geng Huo, PhD,[a] Hirotsugu Notsuda, MD, PhD,[a,b] Zhenhao Fang, PhD,[a,c] Ningdi Feng Liu, BScH,[a,c] Teklab Gebregiworgis, PhD,[a,c] Quan Li, PhD,[a] Nhu-An Pham, PhD,[a] Ming Li, MD,[a] Ni Liu, MSc,[a] Frances A. Shepherd, MD,[a] Christopher B. Marshall, PhD,[a] Mitsuhiko Ikura, PhD,[a,c] Nadeem Moghal, PhD,[a,*] Ming-Sound Tsao, MD, FRCPC[a,c,d,*]

[a]*Princess Margaret Cancer Centre, University Health Network, Toronto, Ontario, Canada*
[b]*Department of Thoracic Surgery Institute of Development, Aging and Cancer, Tohoku University, Sendai, Japan*
[c]*Department of Medical Biophysics, University of Toronto, Toronto, Ontario, Canada*
[d]*Department of Laboratory Medicine and Pathobiology, University of Toronto, Toronto, Ontario, Canada*

Received 24 December 2020; revised 23 September 2021; accepted 23 September 2021
Available online - 12 October 2021

ABSTRACT

Introduction: Mutations in *BRAF* occur in 2% to 4% of patients with lung adenocarcinoma. Combination dabrafenib and trametinib, or single-agent vemurafenib is approved only for patients with cancers driven by the V600E *BRAF* mutation. Targeted therapy is not currently available for patients harboring non-V600 *BRAF* mutations.

Methods: A lung adenocarcinoma patient-derived xenograft model (PHLC12) with wild-type and nonamplified EGFR was tested for response to EGFR tyrosine kinase inhibitors (TKIs). A cell line derived from this model (X12CL) was also used to evaluate drug sensitivity and to identify potential drivers by small interfering RNA knockdown. Kinase assays were used to test direct targeting of the candidate driver by the EGFR TKIs. Structural modeling including, molecular dynamics simulations, and binding assays were conducted to explore the mechanism of off-target inhibition by EGFR TKIs on the model 12 driver.

Results: Both patient-derived xenograft PHLC12 and the X12CL cell line were sensitive to multiple EGFR TKIs. The *BRAF^{G469V}* mutation was found to be the only known oncogenic mutation in this model. Small interfering RNA knockdown of BRAF, but not the EGFR, killed X12CL, confirming BRAF^{G469V} as the oncogenic driver. Kinase activity of the BRAF protein isolated from X12CL was inhibited by treatment with the EGFR TKIs gefitinib and osimertinib, and expression of BRAF^{G469V} in non–EGFR–expressing NR6 cells promoted growth in low serum condition, which was also sensitive to EGFR TKIs. Structural modeling, molecular dynamic simulations, and in vitro binding assays support BRAF^{G469V} being a direct target of the TKIs.

Conclusions: Clinically approved EGFR TKIs can be repurposed to treat patients with non-small cell lung cancer harboring the *BRAF^{G469V}* mutation.

Keywords: Tyrosine kinase inhibitor; NSCLC; Therapeutics; Off-target; Drug repurposing

Introduction

Activating mutations in protein kinases are widely implicated in cancer pathogenesis, and many highly selective kinase inhibitors that target these mutations have been developed and approved for cancer treatment.[1]

*Corresponding author.

Drs. Huo and Notsuda contributed equally to this work.

Disclosure: Dr. Tsao reports receiving research grant (to institution) and consultancy honorarium from AstraZeneca. The remaining authors declare no conflict of interest.

Address for correspondence: Nadeem Moghal, PhD or Ming-Sound Tsao, MD, FRCPC, Princess Margaret Cancer Research Tower, 101 College Street Toronto, ON M5G 1L7, Canada. E-mail: nadeem.moghal@uhnresearch.ca; ming.tsao@uhn.ca

ISSN: 1556-0864
https://doi.org/10.1016/j.jtho.2021.09.008

Non-small cell lung cancer (NSCLC) is the leading cause of cancer-related death worldwide,[2] and mutations in *BRAF*, which encodes a serine/threonine kinase in the RAS-MAPK signaling pathway, have been identified in 2% to 4% of NSCLC, mainly in lung adenocarcinoma.[3–5] Approximately 30% of *BRAF* somatic mutations in NSCLC involve the V600 codon.[4] Responses to V600 mutant-specific BRAF inhibitors (vemurafenib and dabrafenib) have been observed in patients with NSCLC, and dabrafenib, in combination with a MEK inhibitor trametinib, has been approved by the Food and Drug Administration (FDA) for first-line treatment of *BRAF* V600E-positive patients.[6] Nevertheless, this therapy is not effective in patients harboring non–V600-mutated tumors.[5,7]

To investigate new treatment opportunities for tyrosine kinase inhibitors (TKIs) in NSCLC, we screened several approved TKIs against an unbiased cohort of patient-derived tumor xenografts (PDXs), which capture the diversity of genetic alterations found in patient tumors.[8] Unexpectedly, we found that a PDX model harboring $BRAF^{G469V}$, which is one of the more prevalent non-*V600 BRAF* mutations in NSCLC,[4,9] responded to EGFR TKIs. Mechanistic studies supported by structural modeling strongly suggest that although the G469V substitution activates BRAF, it also renders it sensitive to direct targeting by the EGFR TKIs. This finding may provide an accelerated pathway for novel therapy in patients bearing noncanonical (non-V600) *BRAF*-mutated tumors.

Materials and Methods

PDX and Matching Cell Line

PDX model 12 (PHLC12) was established from a surgically resected lung adenocarcinoma, using protocols approved by The University Health Network Human Research Ethics Board (09-0510) and Animal Care Committee, as previously described (PubMed identifier: 26124487). Tumor was grown in nonobese mice with diabetes and severe combined immune deficiency bred in our institutional animal facility. The mice were housed under sterile conditions and given autoclaved food and water. Cell line X12CL was established from PHLC12 tumors at passage 5 and grown in RPMI-1640 with 10% fetal bovine serum (R10 medium). Other cell lines (NCI-H2291 and HCC-827) were obtained from the American Type Culture Collection (Manassas, VA). Authenticity of cell lines was verified using short tandem repeat DNA fingerprinting, and the cells were certified to be mycoplasma free. All drugs used in this study (gefitinib, erlotinib, afatinib, osimertinib, and TAK-632) were purchased from the University Health Network Shanghai, Inc. (Shanghai, People's Republic of China).

Genomic Characterization of Tumor Models

Whole-exome sequencing (WES) was performed using the HiSeq platform (Illumina, San Diego, CA), and copy number variation was evaluated using the HumanOmni 2.5 BeadChip single-nucleotide polymorphism array platform (Illumina, San Diego, CA), as previously described.[10] Details of data analysis are provided in the Supplemental Materials.

Drug Sensitivity Experiments in PDXs

PHLC12 at passages 3 to 8 was used in this study. Tumor fragments of 30 to 50 mm^3 were engrafted subcutaneously into the right flanks of nonobese mice with diabetes and severe combined immune deficiency mice. Once tumors reached approximately 200 mm^3, the mice were randomized into treatment or control groups and started on their respective treatments at day 0. Gefitinib was resuspended in lactate salt buffer (pH 5.2) and dosed at 100 mg/kg. Osimertinib was resuspended in 3:2 ratio of deionized water:1% Tween 80 and dosed at 25 mg/kg. Tumor sizes were measured twice weekly by digital calipers, and volume measurements were calculated by a modified ellipsoid formula most often used for tumor volume estimation[11,12]: volume = length × width × width × 0.5.

Cell Growth and Cell Line Drug Sensitivity Assays

To quantify cell growth after drug or antibody treatment in vitro, the CellTiter 96 AQueous One Solution Cell Proliferation Assay Kit (Promega Corporation, Madison, WI) was used according to the manufacturer's protocol. Cells were seeded in 96-well plates at a density of 3000 cells per well in100 μL R10 medium and incubated for 24 hours before drug treatment. The following day (d0), baseline cell number was quantified and different concentrations of drugs (1 nM, 3 nM, 16 nM, 80 nM, 400 nM, 2 μM, 10 μM) were added to each well in triplicate. Dimethylsulfoxide (DMSO) was the control drug vehicle. After 72 hours of drug incubation (d3), cell growth for the DMSO control (Cd3) and drug-treated (Td3) groups was again quantified. Relative cell viability is defined as (Td3-d0)/(Cd3-d0).

siRNA Knockdown

Small interfering (si) RNAs were purchased from Horizon Discovery (Waterbeach, United Kingdom) and included the following: ON-TARGETplus Non-targeting Control Pool (D-001810-10-05), ON-TARGETplus Human EGFR siRNA SMARTPool (L-003114-00-0005), and ON-TARGETplus Human BRAF siRNA SMARTPool (L-003460-00-0005). They were transfected at a final concentration of 30 nM using lipofectamine RNAiMax (Thermo Fisher Scientific, Waltham, MA) according to

the manufacturer's protocol. HCC827, H2291, and X12CL cells were cultured in R10 medium in 96-well plates at 3000 cells per well in 100 μL for cell growth experiments and seeded in 6-well plates at 300,000 cells per well in 3 mL for biochemical assays. After overnight seeding, cells were transfected with siRNAs for 72 hours, at which point cell growth was quantified in 96-well plates and cells in 6-well plates were lysed for protein extraction.

EGFR Signaling Inhibition by the Anti-EGFR Antibody Cetuximab

For cell growth experiments, X12CL cells were seeded in 96-well plates at 3000 cells per well in 100 μL R10 medium. On the next day, X12CL cells were treated with either 10 μg/mL of the anti-EGFR antibody cetuximab (Hospira Inc., Lake Forest, IL) or a control immunoglobulin G antibody (12000C, Thermo Fisher Scientific), and after 3 days and 7 days, cell growth was quantified.

Western Blotting

Cells were lysed in radioimmunoprecipitation assay (RIPA) buffer (Thermo Fisher Scientific) with protease and phosphatase inhibitors as previously described.[13] Protein was quantified using the bicinchoninic acid assay according to the manufacturer's instructions (Thermo Fisher Scientific, Waltham, MA). Protein was resolved on 10% Mini-PROTEAN TGX gels (Bio-Rad, Hercules, CA) and transferred to 0.2 μm polyvinylidene difluoride membranes using a Trans-Blot Turbo transfer system (Bio-Rad). Membranes were blocked with 5% nonfat dry milk and probed with the following antibodies against BRAF (1:1000, 14814S, Cell Signaling, Boston, MA), EGFR (1:1000, 2232S, Cell Signaling), phosphoryated (p)-ERK (1:1000, 4370S, Cell Signaling), ERK 1/2 (1:1000, 4695S, Cell Signaling), beta-actin (1:2000, 4967S, Cell Signaling), p-MEK (1:1000, 9121S, Cell Signaling), MEK (1:1000, 9122S, Cell Signaling), p-Tyr (1:1000, sc-7020, Santa Cruz Biotechnology, Dallas, TX), and secondary mouse (1:2000, 7076S, Cell Signaling) and rabbit (1:2000, 7074S, Cell Signaling) conjugated immunoglobulin G-horseradish peroxidase. Detection was performed using Amersham ECL Prime Western Blotting Detection Reagent (GE Healthcare, Chicago, IL). Images were acquired with a Bio-Rad ChemiDoc Imager (Bio-Rad), with band intensity quantified using Bio-Rad Image Lab software 6.0.1 (Bio-Rad).

Molecular Dynamic Simulations

Details of molecular dynamic (MD) modeling are provided in Supplementary Materials.

Cell-Free Kinase Assay

X12CL and H2291 cells were lysed in RIPA buffer (Thermo Fisher Scientific) with protease and phosphatase inhibitors. Endogenous BRAF was immunoprecipitated using anti-BRAF antibodies (1:100, 14814S, Cell Signaling) from 200 mg total protein in 200 mL at 4°C overnight. Immunocomplexes were then purified with 20 μL protein A magnetic beads (73778S, Cell Signaling) and washed 5 times with RIPA buffer (Thermo Fisher Scientific, 25 mM Tris–hydrogenchloride pH 7.6, 150 mM sodium chloride, 1% NP-40, 1% sodium deoxycholate, 0.1% sodium dodecyl sulfate). Immunoprecipitates were then resuspended in 20 μL kinase buffer (1 mM adenosine tri phosphate [ATP], 40 mM magnesium chloride, 5 mM EGTA, 1 mM sodium orthovanadate, 25 mM beta-glycerol-phosphate, and 1 mM dithiothreitol). A trial Western blot was run to determine the levels of immunoprecipitated BRAF in each cell line, to standardize the amount of BRAF used in each kinase assay. Immunocomplexes were then incubated with DMSO control or 10 nM gefitinib or osimertinib for 30 minutes at room temperature. Kinase-inactive MEK1 (1 μg/sample) (Millipore, Catalog number 14-420) was then added to each sample as a BRAF substrate and kinase reactions were carried out at 30°C for 30 minutes. Reactions were terminated by boiling in the presence of 5× sodium dodecyl sulfate loading dye for 5 min, and MEK phosphorylation was quantified by Western blotting (9121S and 9122S, Cell Signaling).

Virus Preparation, Transduction, and Stable Cell Line Generation

The *BRAF* lentiviral vector, pHAGE-BRAF, was purchased from Addgene (Plasmid #116719). The G469V mutation was introduced into this plasmid by swapping in the mutated region from pHAGE-BRAF-G469V (Addgene plasmid #116157) using the restriction enzymes PshAI and BamHI. pHAGE-BRAF and pHAGE-BRAF-G469V were then used to make lentiviruses using a three-vector system in 293T cells as previously described.[14] NR6 cells were infected with the lentiviruses as previously described,[13] and stable cells were selected in 2 μg/mL puromycin for 1 to 2 weeks.

Expression and Purification of BRAF in Insect Cells

Details are provided in Supplementary Materials.

Biolayer Interferometry

Details are provided in Supplementary Materials.

Statistical Methods

Statistical analysis was performed with GraphPad Prism software. PDX figures are presented as either

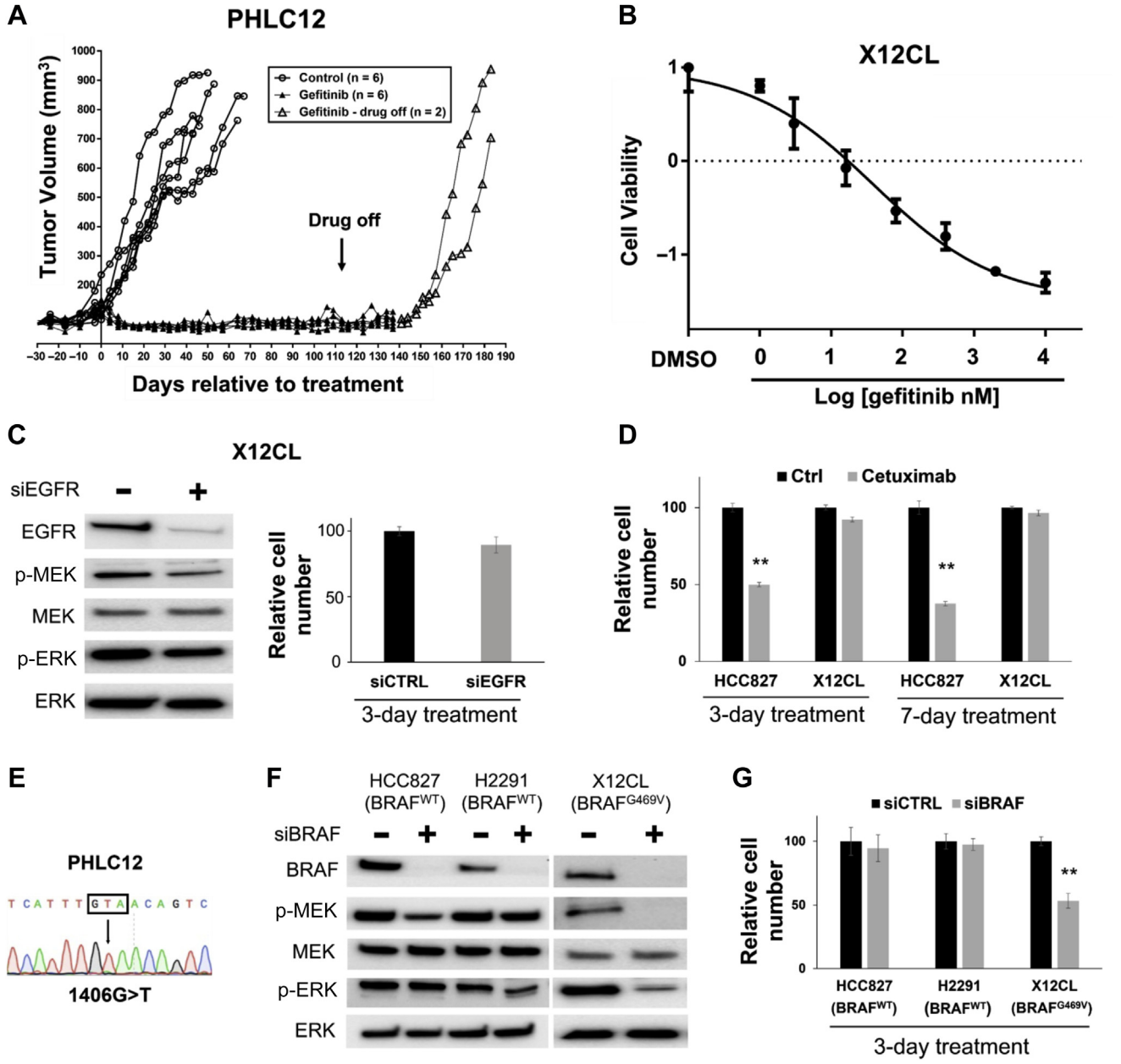

Figure 1. PHLC12 and its derived cell line X12CL are sensitive to gefitinib but driven by BRAF instead of EGFR. (*A*) PHLC12 tumors were initially grown in the absence of drug and then treated commencing at day 0 with either daily oral administration of 100 mg/kg gefitinib (n = 6) or vehicle (n = 6). At the indicated time, drug dosing was stopped for 2 animals within the drug-treated arm. (*B*) Gefitinib kills X12CL cells in vitro. Cells were treated in triplicate with either different doses of gefitinib or Ctrl vehicle. After 3 days, cell growth was quantified and the drug treatment effect on growth was plotted relative to Ctrl. A value below 0 indicates cell killing. Relative viability was calculated as follows: drug day 3 – day 0 / Ctrl day 3 – day 0. Means ± SEM are shown. (*C*) EGFR siRNAs do not inhibit MEK or ERK phosphorylation, nor X12CL growth. X12CL cells were treated in triplicate with either EGFR or Ctrl siRNA for 3 days. EGFR, p-MEK, MEK, p-ERK, and ERK expressions were quantified by Western blotting. Cell number was quantified and expressed relative to Ctrl siRNA, with means ± SEM revealed. (*D*) X12CL cells were treated with 10 μg/mL of the anti-EGFR antibody cetuximab or a Ctrl IgG antibody, and after 3 days and 7 days, cell growth was quantified. $^{**}p < 0.01$ and was calculated by an unpaired *t* test. (*E*) DNA Sanger sequencing chromatogram of PDX12 highlighting the G469V mutation. (*F* and *G*) BRAF siRNA inhibits MEK and ERK phosphorylation and cell growth in X12CL but not HCC827 or H2291 that express WT BRAF. HCC827, H2291, and X12CL cells were treated in triplicate with either BRAF or Ctrl siRNA for 3 days. BRAF, p-MEK, MEK, p-ERK, and ERK expression was quantified by Western blotting. Cell number was quantified and expressed relative to Ctrl siRNA, with means ± SEM revealed. $^{**}p < 0.01$ and was calculated by an unpaired *t* test. Ctrl, control; p, phosphorylated; si, small interfering; WT, wild-type.

individual animals or as means ± SEM. Others results with error bars are represented as the mean ± SEM. Comparison between two groups in the cell-free kinase assay was done using two-tailed paired Student's *t* test. Comparisons between two groups in other experiments were done using two-tailed unpaired Student's *t* test.

Results

The PDX model PHLC12 was established from the resected stage-3A lung adenocarcinoma of a 78-year-old female patient. Growth of this lung cancer xenograft was strongly inhibited by the first-generation EGFR TKI, gefitinib (Fig. 1*A*). Drug withdrawal resulted in tumor regrowth, suggesting PHLC12 is driven by a target of gefitinib. Similarly, the X12CL cell line derived from PHLC12, was killed by gefitinib at concentrations as low as 15 nM (Fig. 1*B*). Both PHLC12 and X12CL exhibited gefitinib sensitivity similar to other models harboring *EGFR* mutations,[15,16] with the cell line responding to doses well below the maximal plasma concentration (C_{max}) in patients receiving the recommended amount of gefitinib (C_{max} = 129 nM).[17]

BRAF^{G469V}-Driven Lung Adenocarcinoma Is Sensitive to the EGFR TKI Gefitinib

Surprisingly, WES of PHLC12 did not identify activating *EGFR* mutations (Supplementary Table 1). In fact, no mutations or copy number gains were detected in any *ERBB* family gene, which includes *EGFR*, *ERBB2*, *ERBB3*, and *ERBB4* (Supplementary Table 2). Because a few patient tumors and cell lines with only wild-type *EGFR* are sensitive to EGFR TKIs,[18–20] we investigated whether X12CL growth is driven by wild-type EGFR. *EGFR* knockdown by siRNA did not affect MAPK signaling or cell growth (Fig. 1*C*), nor did treatment with the anti-EGFR neutralizing antibody, cetuximab (Fig. 1*D*). By contrast, cetuximab inhibited growth of the mutant *EGFR*-driven cell line HCC827 (Fig. 1*D*). These results indicate that wild-type EGFR is not an oncogenic driver in X12CL cells and suggest that gefitinib targets a non-ErbB driver in these cancer cells.

The only mutation identified in PHLC12 WES as oncogenic according to OncoKB[1] (Supplementary Table 1) was a *BRAF* mutation encoding a G469V substitution, which we confirmed by Sanger sequencing (Fig. 1*E*) and has been functionally validated as oncogenic in other models.[7,21] Mutations affecting G469, including *BRAF^{G469V}* and *BRAF^{G469A}*, activate MAP kinase signaling and promote growth factor-independent Ba/F3 cell proliferation.[7,21] *BRAF^{G469V}* is one of the more prevalent non-*V600* *BRAF* mutations in *BRAF*-mutant NSCLC in the American Association for Cancer Research (3.1%)[4] and The Cancer Genome Atlas (8.6%)[9] data sets (Supplementary Table 3) and is also found in other cancer types (Supplementary Table 4). Genome-wide CRISPR dropout screens involving hundreds of cancer cell lines did not identify *BRAF* as a common essential gene (DepMap, https://depmap.org/portal/),[22] which is likely due to signaling redundancy between ARAF, BRAF, and RAF1. Consistent with these data, we confirmed that growth and MAPK signaling of the NSCLC lines HCC827 and H2291 that only harbor wild-type *BRAF* are not inhibited by BRAF siRNA (Fig. 1*F* and *G*). By contrast, X12CL growth and MAPK signaling were inhibited by BRAF knockdown (Fig. 1*F* and *G*). Because we could only detect mutant *BRAF* DNA in PHLC12 from which X12CL cells are derived (Fig. 1*E*), we interpret the knockdown data to indicate that reduction in mutant BRAF^{G469V} causes growth inhibition in X12CL cells. This interpretation is consistent with the lack of effect of targeting wild-type *BRAF* in other cancer cells. Furthermore, X12CL cells were two orders of magnitude more sensitive to TAK-632, a pan-RAF inhibitor that can also target BRAF^{G469V},[7,23,24] than HCC827 lung cancer cells (Supplementary Fig. 1). Together, these data support BRAF^{G469V} being a major oncogenic driver in X12CL cells and PHLC12.

BRAF^{G469V} Is Targetable by Multiple EGFR TKIs

We next evaluated whether other EGFR TKIs inhibit X12CL growth. Both the second-generation EGFR TKI afatinib and the current first-line EGFR TKI osimertinib started to kill X12CL cells at 15 nM (Fig. 2*A*), well below their C_{max} at recommended doses.[25,26] Afatinib and osimertinib (Fig. 2*B* and *C* and Supplementary Fig. 2) also strongly suppressed growth of the PHLC12 xenograft. Because BRAF^{G469V} is not dependent on RAS activity,[7,23] we tested whether BRAF^{G469V} might be directly inhibited by these EGFR TKIs in vitro. Endogenous BRAF^{G469V} was purified from X12CL cells by immunoprecipitation. The immunoprecipitates were verified to be free of EGFR contamination (Fig. 2*D*) and were then used in in vitro kinase assays in either the presence or absence of TKIs. Both gefitinib and osimertinib inhibited BRAF^{G469V} kinase activity toward its natural substrate, MEK (Fig. 2*E*). By contrast, wild-type BRAF purified from H2291 cells was not inhibited by either TKI (Fig. 2*E*). To further validate whether the EGFR TKIs act through BRAF^{G469V} and not the EGFR, we engineered expression of either human BRAF^{WT} or BRAF^{G469V} in murine NR6 fibroblasts that do not express endogenous EGFR[27] (Fig. 2*F* and Supplementary Fig. 3*A*). In 1% serum, parental NR6 and BRAF^{WT}-expressing cells do not grow (Fig. 2*G*). By contrast, BRAF^{G469V} is able to drive growth in 1% serum (Fig. 2*G*), establishing a condition where antagonism of its activity can be discerned by virtue of growth

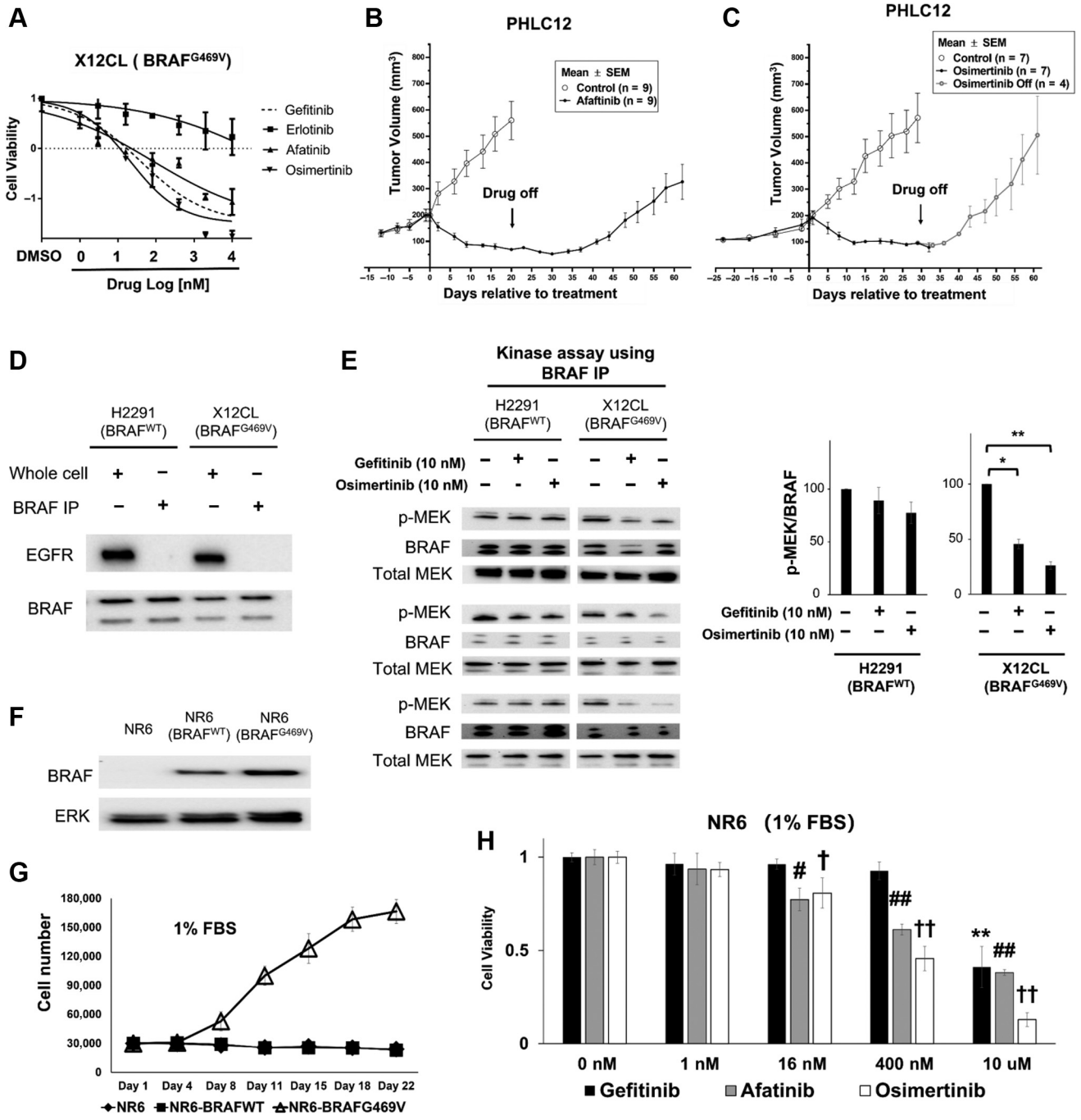

Figure 2. BRAF^{G469V} is targetable by multiple EGFR TKIs. (*A*) Killing of X12CL cells by EGFR TKIs. Cells were treated in triplicate with either different doses of the TKI or control vehicle. After 3 days, cell growth was quantified and the drug treatment effect on growth was plotted relative to control. A value below 0 indicates cell killing. Relative viability was calculated as follows: drug day 3 – day 0 / control day 3 – day 0. Means ± SEM are revealed. (*B* and *C*) PHLC12 growth is inhibited by second- (afatinib) and third- (osimertinib) generation EGFR TKIs. PHLC12 tumors were initially grown in the absence of drug and then treated commencing at day 0 with either daily oral administration of 25 mg/kg afatinib (n = 7) or osimertinib (n = 7) or vehicle. Means ± SEM are revealed. (*D*) WT and G469V BRAF proteins were purified from cancer cells having either wild-type *BRAF* genomic DNA (H2291) or carrying the *BRAF^{G469V}* somatic mutation (X12CL), respectively, using IP. EGFR and BRAF expression was quantified by Western blotting. (*E*) EGFR TKIs inhibit BRAF^{G469V} kinase activity. Purified WT and G469V BRAF proteins were subjected to immune-complex kinase assays in vitro using recombinant MEK as a substrate. Reactions were carried out either in the presence or absence of 10 nM EGFR TKI, with MEK phosphorylation quantified by Western blotting. The histogram depicts quantification of triplicate kinase assays, with data from each cell line independently normalized to their corresponding vehicle-treated controls (means ± SEM). *$p < 0.05$ and **$p < 0.01$, as calculated by paired *t* tests. (*F*–*H*) Growth of NR6 cells that overexpress G469V BRAF is inhibited by EGFR TKIs. (*F*) NR6 cells were infected by lentivirus expressing WT or G469V BRAF. BRAF and ERK expression was quantified by Western blotting. (*G*) NR6 cells that

inhibition. Afatinib, osimertinib, and to a lesser extent, gefitinib, all inhibited growth of $BRAF^{G469}$ cells in 1% serum (Fig. 2*H*). In contrast, in standard 10% serum where growth of $BRAF^{WT}$ cells can be assayed, no concentration of any EGFR TKI inhibited growth, indicating sensitivity to EGFR TKIs tracks with presence of $BRAF^{G469V}$ (Supplementary Fig. 3*B*).

Molecular Modeling Supports EGFR TKIs Directly Targeting $BRAF^{G469V}$

To explore how a TKI with specificity toward the EGFR might be able to also inhibit certain mutant forms of the BRAF serine/threonine kinase, we compared the drug/ligand-bound protein structures of BRAF and EGFR. Owing to the lack of a $BRAF^{G469V}$ structure, we compared the structure of activated $BRAF^{V600E}$ complexed with vemurafenib to that of $EGFR^{L858R}$ complexed with gefitinib. Although they belong to different classes of kinases, the BRAF and EGFR catalytic domains are markedly homologous with highly conserved drug/ligand-binding pockets near the ATP-binding site. This is especially apparent in the phosphate-binding loop (P-loop) and activation segments (Fig. 3*A*), suggesting the potential for some cross-specificity of inhibitor binding. Indeed, discoveries of agerafenib and BGB-283, dual RAF/EGFR inhibitors with similar nM potency for both kinases, support the notion that both kinases can be inhibited by a single scaffold.[28,29] In addition, the chemical structures of gefitinib and the BRAF inhibitor vemurafenib share a similar core comprising bicyclic and fluorophenyl ring moieties (Supplementary Fig. 4*A*). Nevertheless, at least in the context of the $BRAF^{V600E}$ structure, the methoxy adduct on the quinazolin moiety of gefitinib is predicted to cause a mild steric clash with C532 in the BRAF hinge region, suggesting steric constraints may prevent gefitinib from binding both the V600E and wild-type forms of BRAF.

To next investigate whether the G469V substitution could potentially alter the BRAF conformation to facilitate gefitinib binding, we modeled structures of the BRAF-mutant G469V using a crystal structure of wild-type BRAF as a template. Replacement of glycine with valine at position 469 in the P-loop results in an obvious intramolecular steric clash: the valine side chain seems incompatible with normal positioning of the M484 side chain in the kinase α-C-helix (Supplementary Fig. 4*B*). Thus, the G469V mutation must introduce a conformational rearrangement to accommodate valine's bulky side chain, and this is likely to distort the flexible P-loop. We then performed MD simulations to predict changes in protein conformation and ligand coordination that may be caused by the G469V mutation. The MD simulations revealed that the interaction of $BRAF^{G469V}$ with gefitinib was enhanced (with lower interaction energy), whereas that with ATP was reduced (higher interaction energy), relative to wild-type BRAF (Fig. 3*B*–*F*). These results are consistent with the impact of P-loop mutations on ATP affinity of multiple kinases,[30] and because gefitinib is an ATP-competitive inhibitor, they suggest that the G469V mutation may facilitate displacement of ATP by gefitinib to make this BRAF mutant more sensitive to this TKI. The modeling predicted that the G469V substitution substantially alters positioning of the P-loop and enhances its motion (Supplementary Fig. 5), which likely impairs its optimal contacts with the ATP phosphates and could potentially relieve the mild steric constraint observed in the model of gefitinib binding to wild-type BRAF.

G469V Substitution Promotes Binding of EGFR TKIs to BRAF

To determine whether the G469V substitution does indeed facilitate binding of EGFR TKIs to BRAF, we used biolayer interferometry (BLI, Octet) with human $BRAF^{WT}$ and $BRAF^{G469V}$ that were expressed and purified (in complex with endogenous 14-3-3 proteins) from insect cells. Both proteins also had an S365A substitution to prevent phosphorylation of the inhibitory 14-3-3-binding site, but retained 14-3-3 binding, presumably by the stimulatory S729 phosphosite. The S365A mutation was used to destabilize the autoinhibited "closed" conformation and try to shift most of the BRAF species toward the more open active conformation,[31] which is the state that most likely interact with the TKIs in vivo. After immobilization of BRAF protein on biosensors, the sensors were dipped into wells containing EGFR TKIs to monitor association, followed by buffer alone to monitor dissociation (Fig. 4*A* and *B*). Binding of afatinib, osimertinib, and gefitinib was each detected for both WT and mutant BRAF. Nevertheless, $BRAF^{G469V}$ consistently revealed enhanced

overexpress G469V BRAF but not that overexpress WT BRAF, nor parental NR6 cells, were able to grow in 1% FBS. (*H*) Killing of $BRAF^{G469V}$-expressing NR6 cells by EGFR TKIs. Cells were treated in triplicate with either different doses of the TKI or control vehicle in 1% FBS. Medium and drugs were refreshed every 3 days. After 10 days, cell growth was quantified and the drug treatment effect on growth was plotted relative to control. The histogram depicts quantification of triplicate kinase assays, with data from each cell line independently normalized to their corresponding vehicle-treated controls (means ± SEM). Relative viability was calculated as follows: drug day 10/control day 10. #, †$p < 0.01$ and **, ##, ††$p < 0.001$ as calculated by an unpaired *t* test. FBS, fetal bovine serum; IP, immunoprecipitation; p, phosphorylated; TKI, tyrosine kinase inhibitor; WT, wild-type.

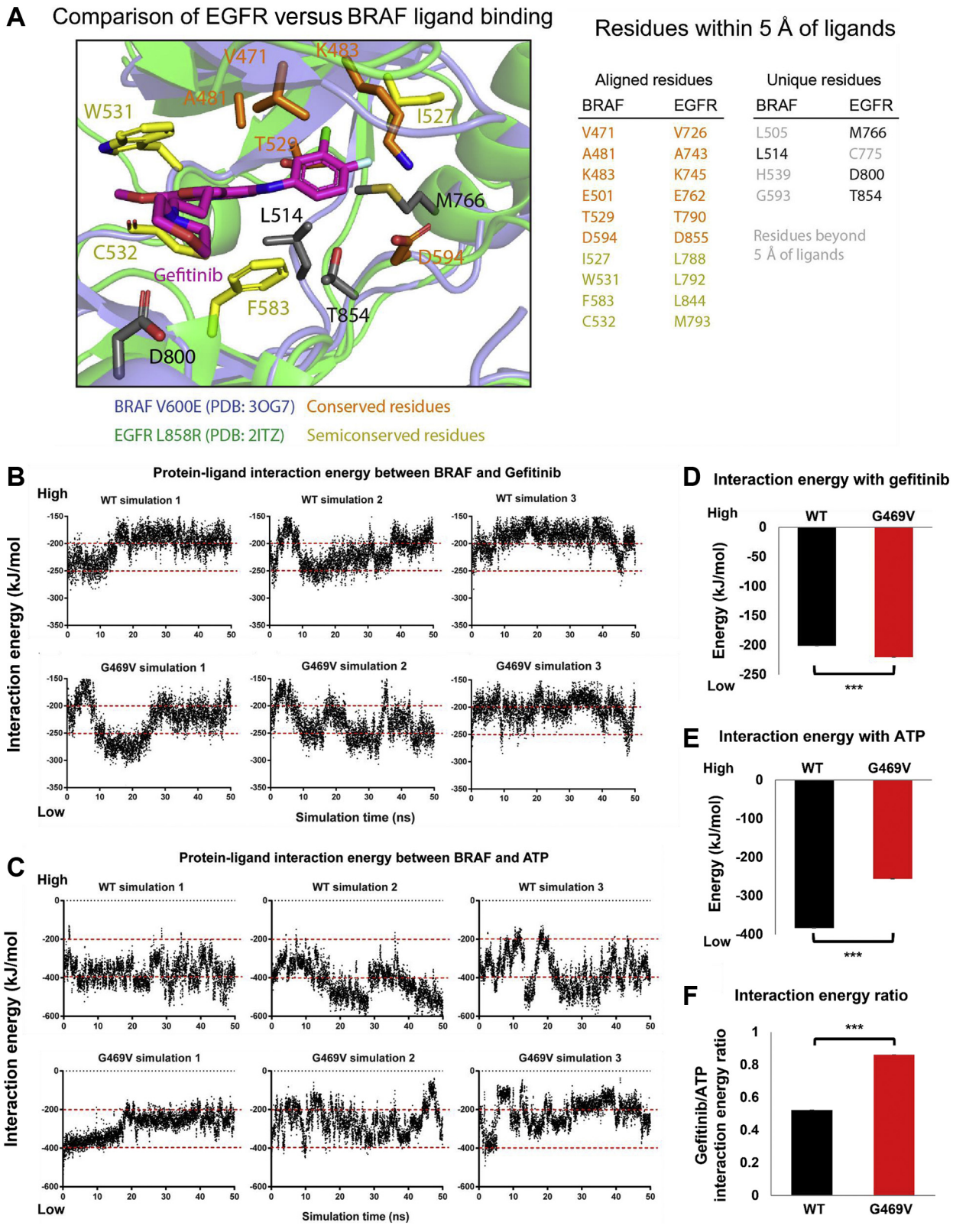

Figure 3. Molecular dynamic simulation supports that BRAF^{G469V} is a target for EGFR TKIs. (*A*) Structural similarity between BRAF and EGFR kinase domains complexed with targeted inhibitors. Overlay of structures of BRAF^{V600E} (blue) cocrystallized with vemurafenib (cyan, PDB: 3OG7) and EGFR^{L858R} (green) cocrystallized with gefitinib (magenta, PDB: 2ITZ). Residues within 5 Å of ligands are shown in stick mode, with those fully conserved between BRAF and EGFR colored in orange. Semiconserved residues are colored in yellow and unique residues that seem in only one kinase ligand pocket are colored in black. Conserved residue pairs are labeled using the BRAF sequence, except for three unique EGFR residues, M766, D800 and

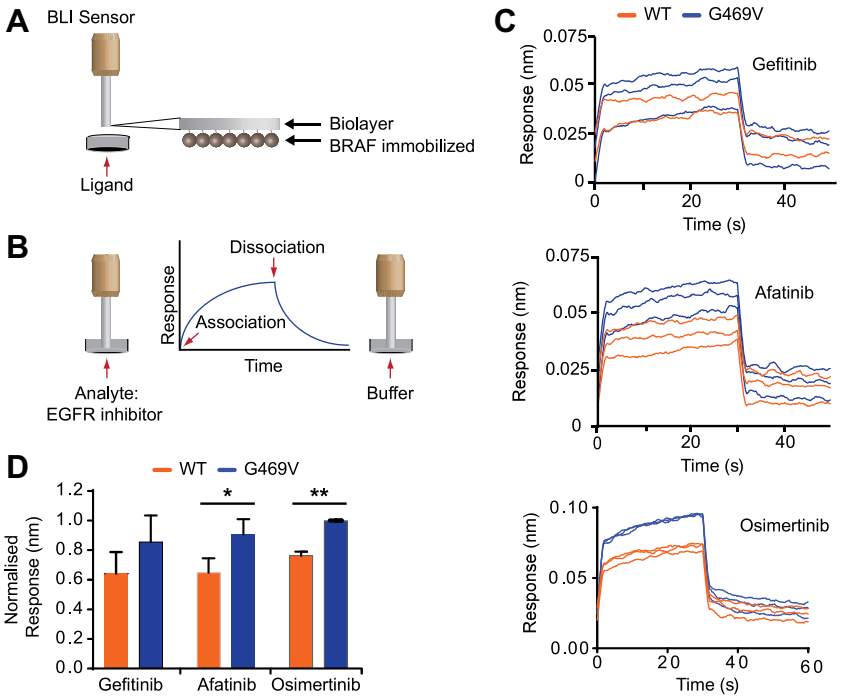

Figure 4. The G469V mutation enhances the binding of TKIs to BRAF. (*A* and *B*) BLI assay setup. Purified recombinant full-length human BRAF constructs (G469V and WT 1) were separately immobilized by means of amine coupling to ARG2 biosensors, which were then dipped into wells containing 25 μM of inhibitor (t = 0 s) to monitor association, followed by buffer alone (t = 30 s) to monitor dissociation. (*C*) BLI response curves revealing binding of gefitinib, afatinib, and osimertinib, respectively, to G469V BRAF (blue) and its WT counterpart (orange). Three representative experiments are found for each condition. (*D*) Normalized binding responses to different TKIs for G469V BRAF relative to WT. Error bars represent SD across three replicates. *$p < 0.05$ and ** $p < 0.001$ as calculated by an unpaired *t* test. Note: both constructs contain an N-terminal maltose-binding protein tag and an S365A substitution. BLI, biolayer interferometry; TKI, tyrosine kinase inhibitor; WT, wild-type.

binding relative to WT, as indicated by the amplitude of their respective BLI response curves (Fig. 4*C*). This enhanced binding to mutant BRAF reached significance for afatinib and osimertinib when comparing differences in the normalized binding responses from the replicates (Fig. 4*D*). The binding events in this assay seemed relatively weak, requiring TKI concentrations greater than 1 μM for detection, which prevented the determination of reliable Kd values. The weak interactions with the TKIs could reflect technical constraints of the in vitro binding assay. Detecting the binding of small molecules to BRAF in BLI is complicated by its large size and long intrinsically disordered regions. Furthermore, it is possible that the nonphysiological conditions and immobilization required for BLI impaired BRAF stability and accessibility of small molecules to the kinase domain, as compared with cell-based assays. Nevertheless, the BLI binding assays support EGFR TKIs having a propensity to bind BRAF, which is enhanced by the G469V mutation.

Discussion

In this study, we provide evidence that certain EGFR TKIs, such as gefitinib, afatinib, and osimertinib, can directly inhibit the G469V BRAF mutant to suppress lung cancer growth. These TKIs kill the tumor cells in vitro at concentrations well below their plasma C_{max} observed with typical patient dosing[17] and inhibit growth of a $BRAF^{G469V}$-driven lung cancer PDX at doses typically used to treat tumors with sensitizing EGFR mutations.[15,16] At

T854. Key structural elements including the AS, P-loop, αC helix, and hinge are indicated. (*B–F*) MD simulations predict that $BRAF^{G469V}$ forms more stable complexes with gefitinib and less stable complexes with ATP, as compared with WT BRAF. Protein-ligand interaction energy was calculated for WT and G469V BRAF in complex with (*B*) gefitinib or (*C*) ATP in three independent MD simulations of 50 nanoseconds. The interaction energy is the sum of short-range Coulombic interaction energy and Lennar-Jones energy. Interaction energies calculated from the MD simulations were averaged over 50 nanoseconds for 15,000 different structures and are revealed for gefitinib (*D*) and ATP (*E*) as means ± SEM. (*F*) Ratios of the interaction energies of gefitinib and ATP with WT and G469V BRAF (gefitinib/ATP) were calculated using a bootstrapping approach (see Methods). ***$p < 0.001$ as calculated by unpaired *t* tests. AS, activation segment; ATP, adenosine tri phosphate; MD, molecular dynamic; P-loop, phosphate-binding loop; TKI, tyrosine kinase inhibitor; WT, wild-type.

first glance, it seems surprising that TKIs as structurally distinct as gefitinib and osimertinib can both inhibit $BRAF^{G469V}$, especially because for the EGFR, a major part of the mechanism of osimertinib inhibition involves covalent linkage to C797 in the kinase domain, which is missing in BRAF.[32] Nevertheless, C797 (or its equivalent in other kinases) is not the only determinant of the activity of osimertinib. Noncovalent interactions also play a major role in the inhibitory activity of osimertinib toward the EGFR, which are enhanced when the EGFR kinase domain is in an active state, as caused by the L858R oncogenic mutation.[33] Furthermore, osimertinib has been found to have considerable inhibitory activity toward some kinases that do not even have an equivalent cysteine residue in the ATP-binding site (e.g., ACK1, MLK1, and MNK2).[32] In addition, our data support that there are some differences between how gefitinib and osimertinib interact with $BRAF^{G469V}$. In the PHLC12 PDX model and its X12CL cell line, gefitinib and osimertinib are similarly effective. Nevertheless, in $BRAF^{G469V}$-overexpressing cells, osimertinib was more effective than gefitinib. Because purified BRAF from different sources also revealed differential sensitivity to distinct TKIs ($BRAF^{G469V}$ from X12CL cells was similarly sensitive to gefitinib and osimertinib whereas $BRAF^{G469V}$ from insect cells bound osimertinib better than gefitinib), it is possible that cell-specific factors affecting a modification on BRAF, such as phosphorylation, affect interactions with TKIs, such as gefitinib. Despite there being distinct nuances to how some EGFR TKIs interact with $BRAF^{G469V}$, the overall results support the notion that the G469V mutant form of BRAF is a specific and direct target of structurally distinct classes of EGFR inhibitors.

Development of specific protein kinase inhibitors has revolutionized cancer care.[34,35] Nevertheless, here, we provide evidence that "off-target" inhibition by some kinase inhibitors may also significantly affect cancer treatment. Although the anti-EGFR antibody cetuximab is thought to work "on-target" by the EGFR to inhibit growth of colorectal cancers driven by class III (kinase-dead) BRAF mutants,[36] here we provide evidence that inhibitors of the EGFR kinase domain can act off-target to suppress lung cancer growth. This off-target inhibition by EGFR TKIs on $BRAF^{G469V}$ may be facilitated by fundamental structural properties shared between activated forms of protein kinases. Indeed, using in vitro kinase assays, oncogenic mutations in other kinases have also been found to increase sensitivity to off-target inhibition. For example, the activated mutants $PDGFR\alpha^{T674I}$ and $ABL1^{Q252H}$ are inhibited by the EGFR TKI erlotinib and the Cdk1/Cdk2/GSK-3β inhibitor alsterpaullone, respectively, and similar to $BRAF^{G469V}$, inhibition is confined to specific mutant forms of these kinases.[37] Similarly, even the sensitivity of BRAF to kinase inhibitors can be further diversified by specific mutations other than G469V. As compared with wild-type BRAF, the kinase activities of $BRAF^{V599E}$ and $BRAF^{V600E}$ are much more sensitive to the p38/MAPK inhibitor SB-202190, and the RET TKI, AST-487, respectively.[37,38] Although the specific reasons for each off-target interaction with a kinase inhibitor are not known, the collective data suggest that by stabilizing the activated conformation of the kinase domain, which is more structurally conserved than inhibited conformations, some oncogenic mutations facilitate off-target binding of inhibitors that have a propensity to bind activated conformations.[38] Also, some mutations (e.g., P-loop mutations such as G469V) weaken the coordination of ATP,[30] thus favoring docking of ATP-competitive inhibitors, such as EGFR TKIs, that do not contact P-loop residues. Given the striking specificity of these off-target effects, distinct conformational features created by unique mutations must also contribute to the potency of off-target inhibition by specific drugs.

Current approved targeted inhibitors for BRAF-driven lung cancers include dabrafenib and vemurafenib, which are only effective toward RAS-independent signaling driven by active monomeric (i.e., class I) mutants (primarily codon V600 mutants).[5,7,23] Nevertheless, in patients with lung cancer, approximately 70% of *BRAF* mutations are non-V600 mutations,[4] leaving these patients without an approved targeted therapy. The G469V and G469A mutants are class II mutants, which signal as RAS-independent dimers.[7,23] Because dabrafenib and vemurafenib only inhibit one protomer in a dimer, these drugs are not effective against these mutants.[7,23] Some newer inhibitors (e.g., TAK-632 and BGB-659, which are designated type II) bind monomeric BRAF and both protomers of a RAF dimer and thus inhibit class I and class II BRAF mutants.[7,23,24] Because these new RAF inhibitors also target wild-type RAF dimers in normal cells, there is some concern that they may have a narrower therapeutic index than type I inhibitors.[23] PLX8394 is another type of BRAF inhibitor that disrupts formation of BRAF homodimers and BRAF/CRAF heterodimers, but not CRAF homodimers, suggesting it might have a wider therapeutic index than type II inhibitors.[23] Nevertheless, to date, none of these classes of drugs have yet received FDA approval for non-V600E BRAF-mutant–driven cancers. In this study, we identify multiple FDA-approved EGFR TKIs with validated safety profiles as unexpected therapeutics that can immediately be tested in clinical trials of patients with cancers (NSCLC and other cancers) harboring $BRAF^{G469V}$ mutations. Furthermore, this finding highlights the utility of drug screening in PDXs to potentially discover unexpected therapeutic targets for existing drugs.

CRediT Authorship Contribution Statement

Ku-Geng Huo, Hirotsugu Notsuda, Zhenhao Fang, Nhu-An Pham, Christopher B. Marshall, Mitsuhiko Ikura, Nadeem Moghal, Ming-Sound Tsao: Concept development.

Frances A. Shepherd, Mitsuhiko Ikura, Ming-Sound Tsao: Provision of materials and/or financial support.

Ku-Geng Huo, Hirotsugu Notsuda, Zhenhao Fang, Ningdi Feng Liu, Teklab Gebregiworgis, Ming Li, Ni Liu: Conduct of experiments.

Ku-Geng Huo, Hirotsugu Notsuda, Zhenhao Fang, Ningdi Feng Liu, Teklab Gebregiworgis, Nhu-An Pham, Ming Li, Christopher B. Marshall, Mitsuhiko Ikura, Nadeem Moghal, Ming-Sound Tsao: Data analysis, Interpretation.

Ku-Geng Huo, Zhenhao Fang, Ningdi Feng Liu, Christopher B. Marshall, Mitsuhiko Ikura, Nadeem Moghal, Ming-Sound Tsao: Manuscript writing.

Acknowledgments

This work was supported by the Canadian Institutes of Health Research Foundation grant FDN-148395 (Dr. Tsao) and FDN-410008598 (Dr. Ikura), the Ontario Research Fund Research Excellence grant RE-03–020 (Dr. Tsao), Ontario Premier's Summit Award (Dr. Shepherd), Canadian Cancer Society (Dr. Ikura), and Princess Margaret Cancer Foundation. Dr. Notsuda was supported by the Terry Fox Foundation Special Training Initiative in Health Research at Canadian Institutes of Health Research grant STP53912. Dr. Fang was supported by a Connaught International Scholarship. The authors thank Jessica Weiss for assistance in statistical analysis. This research was enabled in part by support provided by Compute Ontario (https://computeontario.ca/) and Compute Canada (www.computecanada.ca).

Supplementary Data

Note: To access the supplementary material accompanying this article, visit the online version of the *Journal of Thoracic Oncology* at www.jto.org and at https://doi.org/10.1016/j.jtho.2021.09.008.

References

1. Chakravarty D, Gao J, Phillips SM, et al. OncoKB: a precision oncology knowledge base. *JCO Precis Oncol*. 2017;2017: PO.17.00011.
2. World Health Organization. Cancer. https://www.who.int/news-room/fact-sheets/detail/cancer. Accessed August 28, 2021.
3. Alvarez JGB, Otterson GA. Agents to treat BRAF-mutant lung cancer. *Drugs Context*. 2019;8:212566.
4. AACR Project GENIE Consortium. AACR Project GENIE: powering precision medicine through an international consortium. *Cancer Discov*. 2017;7:818–831.
5. Nguyen-Ngoc T, Bouchaab H, Adjei AA, Peters S. BRAF alterations as therapeutic targets in non-small-cell lung cancer. *J Thorac Oncol*. 2015;10:1396–1403.
6. Ettinger DS, Wood DE, Aggarwal C, et al. NCCN Guidelines Insights: Non-Small Cell Lung Cancer, Version 1. 2020. *J Natl Compr Canc Netw*. 2019;17:1464–1472.
7. Yao Z, Torres NM, Tao A, et al. BRAF mutants evade ERK-dependent feedback by different mechanisms that determine their sensitivity to pharmacologic inhibition. *Cancer Cell*. 2015;28:370–383.
8. Huo KG, D'Arcangelo E, Tsao MS. Patient-derived cell line, xenograft and organoid models in lung cancer therapy. *Transl Lung Cancer Res*. 2020;9:2214–2232.
9. Cancer Genome Atlas Research Network, Weinstein JN, Collisson EA, et al. The Cancer Genome Atlas Pan-Cancer analysis project. *Nat Genet*. 2013;45:1113–1120.
10. Wang D, Pham NA, Tong J, et al. Molecular heterogeneity of non-small cell lung carcinoma patient-derived xenografts closely reflect their primary tumors. *Int J Cancer*. 2017;140:662–673.
11. Euhus DM, Hudd C, LaRegina MC, Johnson FE. Tumor measurement in the nude mouse. *J Surg Oncol*. 1986;31:229–234.
12. Jensen MM, Jørgensen JT, Binderup T, Kjaer A. Tumor volume in subcutaneous mouse xenografts measured by microCT is more accurate and reproducible than determined by 18F-FDG-microPET or external caliper. *BMC Med Imaging*. 2008;8:16.
13. Hao J, Zeltz C, Pintilie M, et al. Characterization of distinct populations of carcinoma-associated fibroblasts from non-small cell lung carcinoma reveals a role for ST8SIA2 in cancer cell invasion. *Neoplasia*. 2019;21:482–493.
14. Radulovich N, Leung L, Tsao MS. Modified gateway system for double shRNA expression and Cre/lox based gene expression. *BMC Biotechnol*. 2011;11:24.
15. Jiang Y, Zhao J, Zhang Y, et al. Establishment of lung cancer patient-derived xenograft models and primary cell lines for lung cancer study. *J Transl Med*. 2018;16:138.
16. Yang J, Qin G, Luo M, et al. Reciprocal positive regulation between Cx26 and PI3K/Akt pathway confers acquired gefitinib resistance in NSCLC cells via GJIC-independent induction of EMT. *Cell Death Dis*. 2015;6:e1829.
17. Center for Drug Evaluation and Research, Food and Drug Administration. Clinical pharmacology and biopharmaceutics review(s): application #206995Orig1s000. https://www.accessdata.fda.gov/drugsatfda_docs/nda/2018/208313Orig1s000ClinPharmR.pdf. Accessed August 28, 2021.
18. Hirsch FR, Varella-Garcia M, Bunn PA Jr, et al. Molecular predictors of outcome with gefitinib in a phase III placebo-controlled study in advanced non-small-cell lung cancer. *J Clin Oncol*. 2006;24:5034–5042.
19. Zhu CQ, da Cunha Santos G, Ding K, et al. Role of KRAS and EGFR as biomarkers of response to erlotinib in National Cancer Institute of Canada Clinical Trials Group Study BR.21. *J Clin Oncol*. 2008;26:4268–4275.

20. Bell DW, Lynch TJ, Haserlat SM, et al. Epidermal growth factor receptor mutations and gene amplification in non-small-cell lung cancer: molecular analysis of the IDEAL/INTACT gefitinib trials. *J Clin Oncol*. 2005;23:8081–8092.
21. Ng PK, Li J, Jeong KJ, et al. Systematic functional annotation of somatic mutations in cancer. *Cancer Cell*. 2018;33:450–462.e10.
22. figshare. Broad DepMap 20Q2 public. Dataset. 2020. https://figshare.com/articles/dataset/DepMap_20Q2_Public/12280541/4. Accessed August 28, 2021.
23. Yao Z, Gao Y, Su W, et al. RAF inhibitor PLX8394 selectively disrupts BRAF dimers and RAS-independent BRAF-mutant-driven signaling. *Nat Med*. 2019;25:284–291.
24. Nakamura A, Arita T, Tsuchiya S, et al. Antitumor activity of the selective pan-RAF inhibitor TAK-632 in BRAF inhibitor-resistant melanoma. *Cancer Res*. 2013;73:7043–7055.
25. Center for Drug Evaluation and Research, Food and Drug Administration. Clinical pharmacology and biopharmaceutics review(s): application #201292Orig1s000. https://www.accessdata.fda.gov/drugsatfda_docs/nda/2019/206089Orig1s000ClinPharmR.pdf. Accessed August 28, 2021.
26. Center for Drug Evaluation and Research, Food and Drug Administration. Clinical pharmacology and biopharmaceutics review(s): application 208065Orig1s000. https://www.accessdata.fda.gov/drugsatfda_docs/nda/2013/201292Orig1s000Approv.pdf. Accessed August 28, 2021.
27. Pruss RM, Herschman HR. Variants of 3T3 cells lacking mitogenic response to epidermal growth factor. *Proc Natl Acad Sci U S A*. 1977;74:3918–3921.
28. Rowbottom MW, Faraoni R, Chao Q, et al. Identification of 1-(3-(6,7-dimethoxyquinazolin-4-yloxy)phenyl)-3-(5-(1,1,1-trifluoro-2-methylpropan-2-yl)isoxazol-3-yl)urea hydrochloride (CEP-32496), a highly potent and orally efficacious inhibitor of V-RAF murine sarcoma viral oncogene homologue B1 (BRAF) V600E. *J Med Chem*. 2012;55:1082–1105.
29. Tang Z, Yuan X, Du R, et al. BGB-283, a novel RAF kinase and EGFR inhibitor, displays potent antitumor activity in BRAF-mutated colorectal cancers. *Mol Cancer Ther*. 2015;14:2187–2197.
30. Grant BD, Hemmer W, Tsigelny I, Adams JA, Taylor SS. Kinetic analyses of mutations in the glycine-rich loop of cAMP-dependent protein kinase. *Biochemistry*. 1998;37:7708–7715.
31. Lavoie H, Therrien M. Regulation of RAF protein kinases in ERK signalling. *Nat Rev Mol Cell Biol*. 2015;16:281–298.
32. Cross DA, Ashton SE, Ghiorghiu S, et al. AZD9291, an irreversible EGFR TKI, overcomes T790M-mediated resistance to EGFR inhibitors in lung cancer. *Cancer Discov*. 2014;4:1046–1061.
33. Zhai X, Ward RA, Doig P, Argyrou A. Insight into the therapeutic selectivity of the irreversible EGFR tyrosine kinase inhibitor osimertinib through enzyme kinetic studies. *Biochemistry*. 2020;59:1428–1441.
34. Rossari F, Minutolo F, Orciuolo E. Past, present, and future of Bcr-Abl inhibitors: from chemical development to clinical efficacy. *J Hematol Oncol*. 2018;11:84.
35. Deininger M, Buchdunger E, Druker BJ. The development of imatinib as a therapeutic agent for chronic myeloid leukemia. *Blood*. 2005;105:2640–2653.
36. Yaeger R, Kotani D, Mondaca S, et al. Response to anti-EGFR therapy in patients with BRAF non-V600-mutant metastatic colorectal cancer. *Clin Cancer Res*. 2019;25:7089–7097.
37. Duong-Ly KC, Devarajan K, Liang S, et al. Kinase inhibitor profiling reveals unexpected opportunities to inhibit disease-associated mutant kinases. *Cell Rep*. 2016;14:772–781.
38. Davis MI, Hunt JP, Herrgard S, et al. Comprehensive analysis of kinase inhibitor selectivity. *Nat Biotechnol*. 2011;29:1046–1051.